Dynamics of Ganymede's magnetopause: Intermittent reconnection under steady external conditions

Xianzhe Jia,[1] Raymond J. Walker,[2,3] Margaret G. Kivelson,[1,2,3] Krishan K. Khurana,[2] and Jon A. Linker[4]

Received 2 June 2010; revised 10 September 2010; accepted 20 September 2010; published 2 December 2010.

[1] Magnetic reconnection at the terrestrial magnetopause is frequently intermittent, leading to the formation of localized reconnected flux bundles referred to as flux transfer events (FTEs). It remains unclear whether the intermittency of the process is intrinsic or arises because of fluctuations of solar wind properties. Here we use Ganymede's magnetosphere, which is embedded in a background of field and plasma whose properties vary imperceptibly over time scales pertinent to plasma flow across the moon's magnetosphere, to demonstrate that reconnection is intrinsically intermittent. We run time-dependent global magnetohydrodynamic (MHD) simulations that describe Ganymede's magnetospheric environment realistically and reproduce plasma and field measurements made on multiple Galileo passes by the moon with considerable fidelity. The simulations reveal that even under steady external conditions, dynamic variations associated with magnetic reconnection on time scales of the order of tens of seconds occur over a large region near the upstream magnetopause. The MHD simulations give direct evidence of magnetic reconnection at the magnetopause and reproduce the amplitude and spatial distribution of observed fluctuations of the magnetic field near boundary crossings. The consistency of data and simulations leads us to conclude that even under steady upstream conditions, upstream reconnection is intermittent. The bursty magnetopause structures at Ganymede and the FTEs identified at planetary magnetospheres (Mercury, Earth, and Jupiter) extend the parameter regime for analysis of intermittent magnetopause reconnection. We find that FTE recurrence times decrease with the scale length of the system.

Citation: Jia, X., R. J. Walker, M. G. Kivelson, K. K. Khurana, and J. A. Linker (2010), Dynamics of Ganymede's magnetopause: Intermittent reconnection under steady external conditions, *J. Geophys. Res.*, *115*, A12202, doi:10.1029/2010JA015771.

1. Introduction

[2] Ganymede, the largest satellite in our solar system, earns a unique place among the planetary satellites not only because of its great size but also because it is, so far, the only known satellite to be strongly magnetized [*Kivelson et al.*, 1996]. The intrinsic magnetic field of Ganymede, whose equatorial surface strength (~720 nT) is ~7 times larger than the ambient Jovian field (~100 nT) [*Kivelson et al.*, 1996, 2002], is sufficiently strong to overpower Jupiter's ambient field and consequently stands off the incident Jovian plasma at a distance of about 1 R_G (R_G, radius of Ganymede = 2634 km) upstream of the moon's surface, forming a magnetosphere within Jupiter's magnetosphere [*Kivelson et al.*, 1996; *Gurnett et al.*, 1996; *Williams et al.*, 1997a; *Frank et al.*, 1997]. At Ganymede's orbit ~15 R_J (R_J, radius of Jupiter = 71,492 km), the corotating plasma overtakes the moon from its trailing side because the flow speed is greater than the moon's Keplerian speed. The typical flow speed of the ambient plasma relative to Ganymede is less than the magnetosonic speed. Under such conditions, the corotating plasma directly impinges on and interacts with Ganymede's magnetosphere without being modified by a bow shock such as those that form upstream of planetary magnetospheres. In addition, because of the sub-Alfvénic nature and low plasma β conditions of the typical flow at the moon's orbit, Ganymede's magnetosphere forms a roughly cylindrical shape differing from the bullet-like shape of planetary magnetospheres. The magnetosphere contains a small closed field line region at low latitudes and a large polar cap consisting of field lines that link to Jupiter. Those open field lines in the polar cap are tilted with respect to the background field direction in both hemispheres, forming Alfvén wings that mediate the interaction of Ganymede with the local plasma and with the ionosphere of Jupiter.

[1]Department of Atmospheric, Oceanic and Space Sciences, University of Michigan, Ann Arbor, Michigan, USA.
[2]Institute of Geophysics and Planetary Physics, University of California, Los Angeles, California, USA.
[3]Department of Earth and Space Sciences, University of California, Los Angeles, California, USA.
[4]Predictive Science, Inc., San Diego, California, USA.

0148-0227/10/2010JA015771

[3] Because of the nearly 10° tilt of Jupiter's magnetic axis relative to its spin axis, the external field and plasma conditions around Ganymede's orbit exhibit predictable periodic variations at the nearly 10.5 h synodic period of Jupiter's rotation. Correspondingly, the global configuration of Ganymede's magnetosphere varies in response to the periodic changes in the orientation of the external magnetic field as the moon moves up and down through the Jovian plasma sheet [*Kivelson et al.*, 1998; *Jia et al.*, 2008]. Since Ganymede's intrinsic field is nearly antiparallel to the external field near the equator, magnetic reconnection is believed to be the dominant process that couples the minimagnetosphere with Jupiter's giant magnetosphere. In contrast to the highly fluctuating solar wind with unpredictable variations in plasma and magnetic field conditions, the plasma at Ganymede's orbit imposes external field and plasma conditions that vary slowly with respect to the time required for Jovian plasma to flow across Ganymede's magnetosphere, which is of order minutes. At all times, the Jovian magnetic field remains in a favorable orientation (southward in this case) for reconnection. Therefore, Ganymede's magnetosphere provides us with a good opportunity to investigate the reconnection process in a relatively stable external environment.

[4] During its six close encounters with Ganymede, the Galileo spacecraft has obtained a comprehensive set of field and particle measurements not only in different regions of Ganymede's magnetosphere but also under different external conditions. A detailed review of the flyby geometries and Galileo observations can be found in the work of *Jia* [2009]. Of particular interest here are the two low-latitude passes on the upstream side, the G8 and the G28 passes. During these two flybys, the spacecraft detected what appeared to be large-amplitude fluctuations with periodicities between 20 and 40 s in the magnetic field at the magnetopause crossings [*Kivelson et al.*, 1998]. Whether the observed oscillations were spatial structures or resulted from temporal variations of the magnetopause is not clear based on single spacecraft measurements, although it has previously been proposed that they probably resulted from surface waves caused by the Kelvin-Helmholtz instability on the magnetopause [*Kivelson et al.*, 1998].

[5] By providing global information on field and particle conditions and the time evolution of the magnetosphere, time-dependent global simulations of the magnetosphere can be useful for identifying the origin of the large-scale magnetic fluctuations observed near Ganymede's magnetopause. For the bulk of the ambient plasma near Ganymede with typical energy of ~100 eV [*Kivelson et al.*, 2004], the gyroradius of a heavy ion with mass number 16 in a 100 nT magnetic field is ~50 km, which is less than 1% of the size of Ganymede's magnetosphere. Therefore, an MHD simulation, in which both ions and electrons are treated as fluid, is suitable for studying the global plasma interaction of Ganymede's system. Several MHD simulations, including single-fluid MHD simulations [*Kopp and Ip*, 2002; *Ip and Kopp*, 2002; *Jia et al.*, 2008, 2009] and multifluid MHD simulations [*Paty and Winglee*, 2006], have been carried out to understand the global interaction between Ganymede's magnetosphere and Jovian plasma. While the variations of the global magnetospheric configuration over the synodic period of hours have been investigated in some of the modeling work [*Kopp and Ip*, 2002; *Jia et al.*, 2008], temporal variations of the magnetosphere on time scales shorter than the time for the ambient plasma to convect across the magnetosphere (of the order of minutes) have not yet been discussed. As noted by *Jia et al.* [2009], the simulated magnetopause in our model exhibits dynamic behavior on time scales of the order of tens of seconds, a time scale over which the upstream conditions are effectively constant. Given that our global model [*Jia et al.*, 2009] provides a description of the magnetospheric fields that matches the observations so faithfully, we believe it is capable of representing realistically the behavior at the magnetospheric boundary on scales greater than ion gyroradii. The purpose of this study is to investigate the reconnection process and the associated dynamics of Ganymede's magnetopause under effectively steady external conditions. As will be shown in the following sections, our model results indicate that those short time scale dynamical changes are caused by bursty reconnection in the vicinity of the magnetopause under steady external conditions and that their signatures are consistent with Galileo observations. Lessons for understanding the dynamics of reconnection follow.

[6] The paper is organized as follows. In section 2, we briefly describe the basics of our simulation model. In section 3, we present our simulation results and compare them with observations. A comparison of the FTEs features of Ganymede's magnetosphere with those of planetary magnetospheres is given in section 4, followed by a summary and conclusions in section 5.

2. Simulation Model

[7] In this section, we briefly review some basics of our simulation model. Details of the model can be found in our earlier papers [*Jia et al.*, 2008, 2009]. Our model solves the three-dimensional resistive MHD equations (given by *Jia et al.* [2008]) in spherical coordinates [*Linker et al.*, 1991]. The code utilizes a nonuniform spherical mesh, which imposes high-resolution gridding on such regions of interest as the low-latitude magnetosphere within several R_G of Ganymede's surface. Figure 1 shows the configuration of the spherical grid used in our simulations. Simulations presented here use a numerical mesh that contains $131 \times 132 \times 128$ (r, θ, φ) grid points covering a simulation domain from 0.5 R_G to 40 R_G centered at Ganymede. The grid provides fine resolution within Ganymede's magnetosphere and around the low-latitude magnetopause ($2 \sim 3$ R_G). The finest grid resolution in the radial direction is of order 0.01 $R_G \approx 26$ km in regions close to the moon and the average spatial resolution within the magnetosphere and near the magnetospheric boundaries is about 0.04 $R_G \approx$ 100 km, i.e., of the order of the gyroradius of a heavy ion in the background plasma. As discussed in the work of *Jia et al.* [2008, 2009], such high grid resolution is necessary to capture the signature of plasma currents that produce sharp rotations in the observed magnetic field near the magnetospheric boundaries.

[8] In our model, temporal derivatives in the MHD equations are advanced with leapfrog time differencing combined with a semi-implicit method. The semi-implicit method introduces a term into the momentum equation that effectively modifies the inertia of the short-wavelength

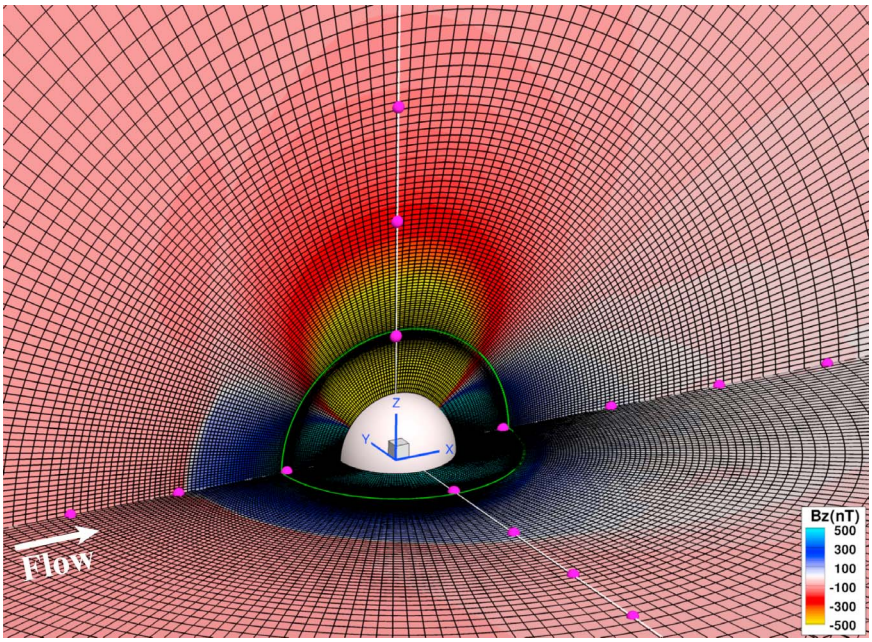

Figure 1. A typical grid distribution in two (r, θ) cuts through the 3-D mesh used in our simulations, viewed from the upstream flank side. These two planes correspond to the XY plane (at Z = 0) and the XZ plane (at Y = 0) in GphiO coordinates, respectively. The three Cartesian axes are labeled with magenta balls every 1 R_G. Color contours of B_z are plotted to show the magnetospheric boundaries. Also plotted are a green circle at radial distance of 1.05 R_G, which corresponds to the inner boundary of the simulation, and a white sphere of radius 0.5 R_G corresponding to the core boundary. Note that high-resolution grids are placed near the magnetopause and magnetotail and close to the moon.

modes, while accurately treating the long wavelengths, enabling the time step to exceed the Courant-Friedrichs-Lewy (CFL) limit for Alfvén and magnetosonic waves. The semi-implicit scheme achieves efficiency by removing short-wavelength high-frequency oscillations. Details about the semi-implicit scheme and examples of its applications to other simulation problems can be found in the work of *Schnack et al.* [1987], *Mikić and Linker* [1994], and *Linker et al.* [1999].

[9] Three boundaries are significant in setting the simulation: the core boundary (at r = 0.5 R_G), the inner boundary (at r = 1.05 R_G) and the outer boundary (at r = 40 R_G). It has been suggested that Ganymede most likely contains a metallic core of radius 0.15 ~ 0.5 R_G that sustains the moon's internal magnetic field [*Anderson et al.*, 1996; *Schubert et al.*, 1996]. Therefore, at the core boundary, the magnetic flux corresponding to Ganymede's internal magnetic field [*Kivelson et al.*, 2002] is set and remains fixed in time. The outer boundary is treated differently in the upstream and downstream regions. At the upstream outer boundary, plasma and field parameters appropriate to regions near Ganymede's orbit at the times of each of the Galileo flybys are specified with constant values corresponding to Galileo observations and fixed in time. At the downstream outer boundary, a nonreflecting boundary condition based on the gas characteristic equation [*Hedstrom*, 1979] is applied and plasma is free to leave the simulation domain at this boundary. To minimize the boundary effects that may be caused by neglecting the magnetic field in the characteristic boundary conditions, the outer boundary is placed far (= 40 R_G) from the region of interest and the run is cut off before any disturbances reflected from the boundary can affect the interior solution.

[10] In developing a global model that can realistically describe Ganymede's magnetosphere, we found that the solutions are extremely sensitive to the boundary conditions imposed at the inner boundary (Ganymede's ionosphere). Several different approaches have been used in specifying the boundary conditions at the inner boundary. In the model of *Jia et al.* [2008], the inner boundary was treated as a highly conducting obstacle just above Ganymede's surface. Although the model presented there produced a magnetosphere that was, in general, consistent with the Galileo magnetic field observations, the simulated magnetosphere was smaller than that inferred from the observations. Later in the work of *Jia et al.* [2009] (hereinafter referred to as Jia09), we demonstrated how our model can be improved by adopting inner boundary conditions that take the local magnetic field into account. The improved boundary condition is applicable for a body surrounded by an ionosphere with finite Pedersen conductance (most likely to be the case for Ganymede). We compared output from runs using different inner boundary conditions and thereby elucidated the sensitivity of the results of the global simulations to the imposed boundary conditions. The improved boundary condition couples convection in Ganymede's ionosphere with that in its magnetosphere in a self-consistent way, and produces a convincing picture of global plasma convection throughout Ganymede's magnetosphere.

[11] An additional refinement used in the Jia09 model was to specify the electric conductivity in different regions of the simulation domain, including the moon's interior, iono-

Table 1. Simulation Parameters for the G8 and G28 Flybys[a]

	G8	G28
M_x (nT)	−18.0	−19.3
M_y (nT)	51.8	17.0
M_z (nT)	−716.8	−716.8
B_y^{bk} (nT)	−6	77
B_z^{bk} (nT)	−77	−76
v_{flow} (km/s)	140	140
ρ (amu/cm^3)	56	28
P (nPa)	3.8	1.9

[a]M_x, M_y, and M_z are the coefficients of the first-order internal moment of Ganymede including both the permanent dipole moment and the induced field in GphiO coordinate system [*Kivelson et al.*, 2002]. Refer to text for the definition of GphiO coordinates. B_y^{bk} and B_z^{bk} are the $\hat{y}$ and $\hat{z}$ components of the background Jovian field in GphiO coordinates. The $\hat{x}$ component B_x^{bk}, which is a minor component compared to B_y^{bk} and B_z^{bk}, is neglected in the simulations as an approximation. Also, v_{flow}, ρ, and P denote the flow speed, mass density and thermal pressure of the background plasma, respectively.

sphere and magnetosphere, in order to reflect realistic conditions suitable for Ganymede. Of particular pertinence to the dynamics of Ganymede's magnetospheric boundaries was the use of an anomalous resistivity model, which was introduced in order to properly model magnetic reconnection in a global MHD simulation. Recent simulation studies of the reconnection process, such as the GEM Reconnection Challenge (a summary of results is given by *Birn et al.* [2001]) and the "Newton Challenge" [*Birn et al.*, 2005], compared details of the reconnection process including the X line geometry and the reconnection rate obtained from different numerical models including resistive MHD, Hall-MHD, hybrid simulations and fully kinetic particle-in-cell (PIC) codes. In general, these studies found that full particle, hybrid, and Hall-MHD simulations lead to the same fast reconnection rates, independent of the dissipation mechanism. On the other hand, resistive MHD simulation with uniform resistivity or with only numerical resistivity tends to obtain a slower reconnection rate, which depends on the value of the resistivity. However, it is found that resistive MHD simulations can obtain similar fast reconnection rate if a spatially localized enhanced resistivity [*Birn and Hesse*, 2001; *Birn et al.*, 2005] or a current-dependent resistivity [*Otto*, 2001] is used. Moreover, as shown by *Birn et al.* [2005], the configuration of the reconnection region, in general, appears to be similar between resistive MHD simulations with spatially localized resistivity and Hall MHD and PIC simulations. To investigate the behavior of Ganymede's magnetopause under external conditions favorable for reconnection in a global context, a current-dependent resistivity model has been adopted in our global MHD model (Jia09). The use of the anomalous resistivity model, which is switched on only in regions with strong localized currents, eliminated unphysical convection patterns and also made fast reconnection possible on the magnetopause (across which oppositely oriented magnetic fields generate strong magnetic shear).

[12] We note that the dynamic behavior of the magnetopause on short time scales develops only when anomalous resistivity is used in the simulation. In an ideal MHD run with only numerical resistivity arising from finite differencing, reconnection on the magnetopause occurs less often with a relatively low reconnection rate compared to that in the case with spatially localized resistivity. In a resistive MHD run with uniformly distributed resistivity, reconnection on the magnetopause tends to be steady and the high resistivity causes the magnetopause to become diffusive. The dependence of the behavior of reconnection on the resistivity model in our code is, in general, consistent with the findings obtained from other simulation studies of reconnection [*Birn and Hesse*, 2001; *Birn et al.*, 2001; *Otto*, 2001; *Birn et al.*, 2005]. In our case, however, the results produced by models with either uniform resistivity or only numerical resistivity are not consistent with the Galileo magnetic field observations shown in the section 3.

[13] Although the anomalous resistivity model adopted in the present study is an oversimplified one that mimicks the dissipation in the diffusion region around the reconnection site, it not only provides a representation of the magnetopause configuration in good agreement with the observations, but also seems to give an improved representation of physical processes occurring throughout Ganymede's magnetosphere as demonstrated in Jia09. With the improvements described above, the new model in Jia09 gives very satisfactory agreement with the magnetic field and plasma observations for one close pass (G8) upstream of Ganymede. The identical changes were used in simulations of all other Galileo passes through the Ganymede system and proved most satisfactory in representing all available magnetic field and particle measurements, thereby demonstrating that our MHD model with appropriate boundary conditions can provide a realistic description of Ganymede's magnetospheric environment.

[14] The initial setup of the simulation contains a uniform flow with a specified plasma density, pressure and flow velocity, and a uniform background field superposed on Ganymede's internal field given by *Kivelson et al.* [2002]. The upstream external conditions are inferred from Galileo observations for each of the passes. The internal field of Ganymede used in the simulations consists of two parts, a permanent dipole and a time-varying component due to induction that varies in response to changes of the external field. Specifics of the initial conditions including the upstream field and plasma conditions used to simulate the two Galileo flybys (G8 and G28) presented in this paper are listed in Table 1.

[15] In the following, we present simulation results output from the Jia09 model with a focus on temporal variations of the magnetopause associated with magnetic reconnection. The Galileo observations and our simulation results shown below are presented in a Ganymede-centered Cartesian coordinate system (so-called "GphiO" coordinates), where $\hat{X}$ is along the ambient flow direction, $\hat{Z}$ is parallel to Jupiter's spin axis and $\hat{Y}$ completes right-hand system with positive pointing toward Jupiter (see Figure 1).

3. Simulation Results and Their Comparisons With the Galileo Observations

[16] As mentioned above, on the two low-latitude passes on the upstream side, the G8 and G28 flybys, the Galileo spacecraft detected what appeared to be large-amplitude waves in the magnetic field at the magnetopause crossings. Such fluctuations are seen in the data plotted in Figure 2b. In Figure 2b, the large magnetic field fluctuations with peri-

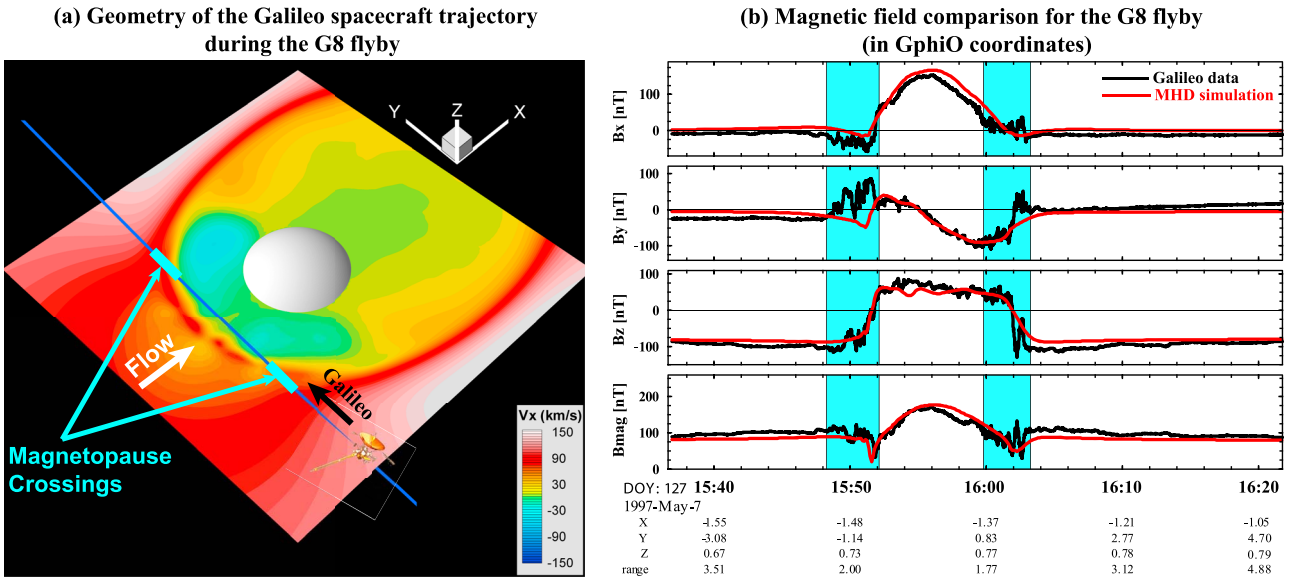

Figure 2. (a) 3-D geometry of the Galileo spacecraft trajectory during the G8 flyby viewed from above. Color contours of V_x output from the simulation of the G8 flyby clearly delineate the magnetopause boundary in the XY plane in which the spacecraft trajectory approximately lies. Two cyan bars mark the portions of the trajectory where large magnetic field fluctuations were observed by Galileo. (b) Magnetic field comparisons between the simulation results and the Galileo observations for the G8 flyby. Black solid lines are the spacecraft measurements, and red solid traces are extracted from a single time step of our MHD simulation. The locations where large-amplitude magnetic fluctuations are observed during both inbound and outbound magnetopause crossings are marked.

odicities between 20 and 40 s were present both prior to the entry and after the exit from the magnetosphere during the G8 flyby and occur in regions marked with cyan in Figure 2b. Figure 2a shows flow contours from the Jia09 simulation. The flow is discontinuous across most of the magnetopause. The portion of the Galileo trajectory that corresponds to the region marked in cyan in Figure 2b is shown in cyan in Figure 2a and overlaps the magnetopause for the selected time step. A single time step does not reveal the dynamical responses of the modeled system. Thus, in order to understand the nature of the fluctuations in the data, we need to examine a range of time steps in the simulation. Hence, we next turn to an examination of the temporal variations of the simulated magnetosphere and compare them with the Galileo observations including magnetic field and plasma measurements obtained during both the G8 and the G28 flybys. Simulation results used here are extracted from times after the runs have reached quasi-steady states in which the large-scale magnetospheric structure has fully developed and changes little with time but temporal variations on smaller scales continue.

3.1. G8 Flyby

[17] Figure 2a illustrates the geometry of the spacecraft trajectory during the G8 flyby. As noted above, color contours of the V_x output from the simulation of the G8 flyby delineate the magnetopause boundary in the XY plane in which the spacecraft trajectory approximately lies. During this flyby, the spacecraft moved primarily in the $+\hat{Y}$ direction, remaining close to the upstream magnetopause.

[18] In order to investigate the dynamics of the magnetosphere, we next examine the temporal variations of the simulation results. Figure 3 shows the superposition of the traced fields in our simulation of the G8 pass at multiple time steps. Each color-coded trace represents the simulated magnetic field extracted along the spatially fixed Galileo trajectory at one time step in the simulation. It can be clearly seen that the location of the magnetopause, indicated by a minimum in the field strength (B_{mag}) and a sharp rotation in B_z, varies in time. In comparison with the observed magnetic field (black trace), the simulated magnetopause varies across much of the locations where large fluctuations were observed during both the inbound (15:49 ~ 15:52 UT) and the outbound (16:00 ~ 16:03 UT) magnetopause crossings (see Animation S1 of the auxiliary material).[1]

[19] In order to investigate what causes the variations of magnetopause location observed in our simulations, we show in Figure 4 (top four panels) the simulated flow velocities observed along the fixed spacecraft trajectory at multiple time steps. It is found from Figure 4 that in the simulation, the magnitude and the location of the peak flow speed vary in time, consistent with the observed variations in the simulated magnetic fields shown in Figure 3. Because magnetic reconnection imposes fast outflows from a reconnection site, we take the fast flows in regions near the magnetopause (mainly in the northward direction, $+V_z$ with speed of >200 km s^{-1}) as evidence of reconnection. The Alfvén

[1] Auxiliary materials are available in the HTML. doi:10.1029/2010JA015771.

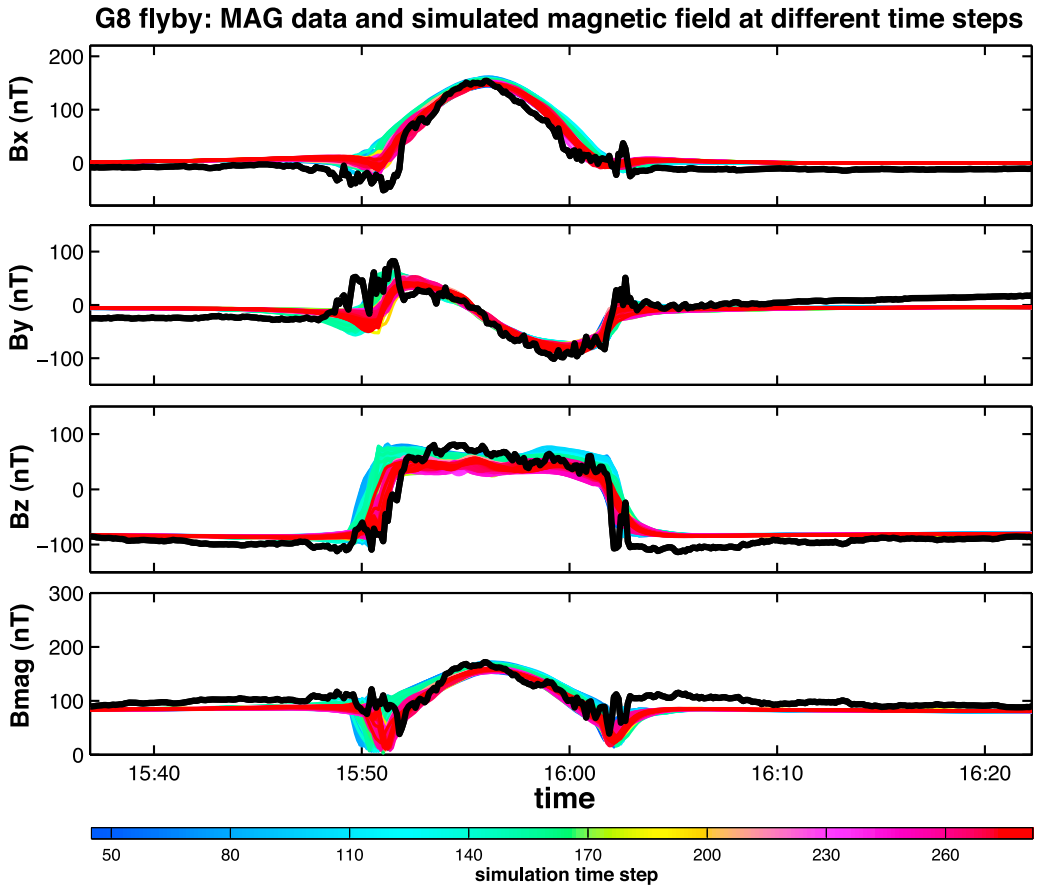

Figure 3. Superposition of the traced magnetic fields (in GphiO coordinates) along the spatially fixed G8 trajectory at different time steps in our simulation. The black solid traces represent the Galileo magnetometer observations. Simulation traces are color coded with their corresponding simulation time steps according to the bottom color bar. Consecutive time steps are separated by ~2 s.

speed of the background flow is of order 200 km s^{-1}. The simulated fast flows whose speed is of order the inflow Alfvén speed are consistent with what is expected for flows initiated by reconnection.

[20] Another feature of the simulated flows is the slowly varying minimum speed. The incident flow speed decreases as it approaches the magnetopause as if there were no magnetopause reconnection. It appears that the bursty fast flows are superimposed on a flow that is slowed near the magnetopause both inbound and outbound. Given that the background flow speed near the magnetopause is <100 km s^{-1} in the absence of reconnection, an enhancement of flow speed of ~200 km s^{-1} associated with magnetopause reconnection produces roughly a factor of 3 increase in flow speed and nearly an order of magnitude increase in the plasma flow energy.

[21] At present, velocity moment data from the Galileo Plasma Subsystem (PLS) are not available from the Planetary Data System (PDS), but ion energy spectrograms are. Figure 4 (bottom) shows such a spectrogram obtained during the G8 flyby. Ion counting rates increase near both the inbound and the outbound magnetopause crossings and there is some energization of particles during the outbound crossings. In addition to the intense intermittent peaks of counting rates, the observed ion counting rates appear to exhibit a secondary peak at lower energies. The energy of the secondary peak decreases with distance from the magnetopause, consistent with slowing of the background flow in the simulation. Also shown in Figure 4 (bottom; as a black dashed trace) is the flow energy of heavy ions (with mass/charge = 16) obtained from the simulated bulk flow speeds extracted from a single time step of the simulation when bursty flows were absent near the magnetopause. As the black dashed trace roughly matches the energies at which the secondary peak in ion counting rates are present both prior to the entry and after the exit from the magnetosphere, it can be considered as a reasonably good representation of the flow energy variation that would have been seen along the spacecraft trajectory in the absence of magnetopause reconnection. In comparison with the model predicted background flow speeds, the PLS spectrogram shows that near the magnetopause, the energies of the peak ion counting rates are higher than the background flow energy by about an order of magnitude just as noted in the simulation. Therefore, those particles with energies above the flow energy of the background corotating plasma observed by the PLS near the magnetopause crossings are likely to be produced by fast flows associated with recon-

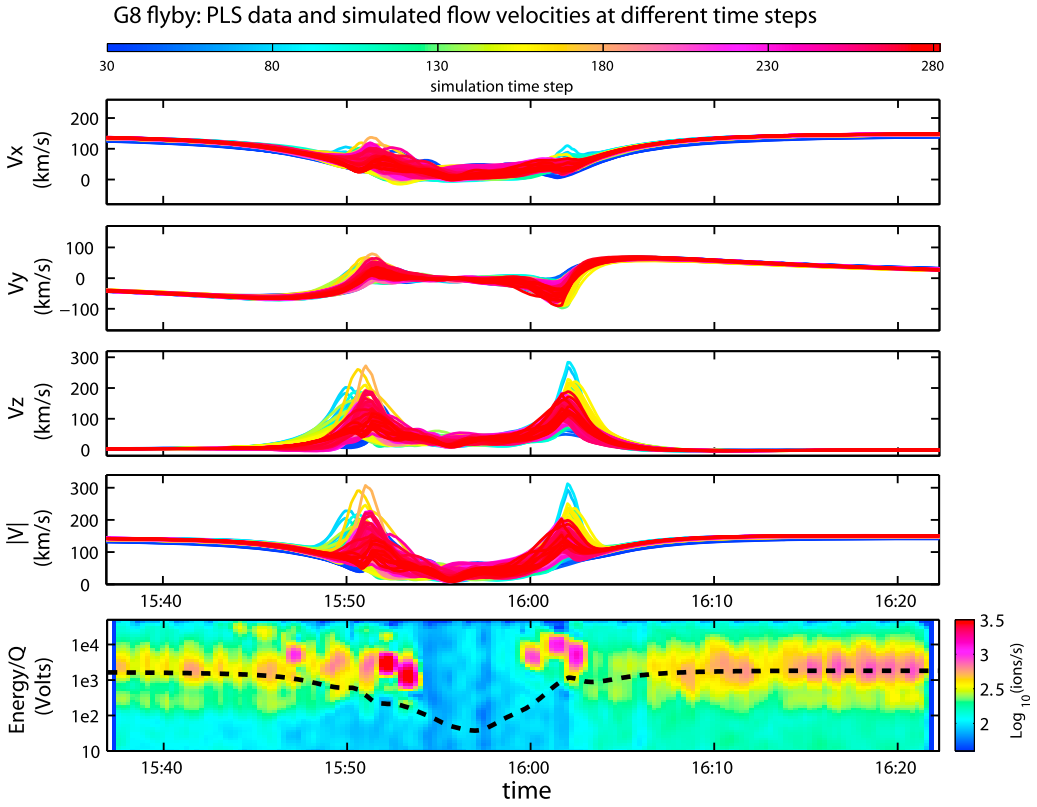

Figure 4. Superposition of the traced velocities (in GphiO coordinates) along the spatially fixed G8 trajectory at different time steps in our simulation. Simulation traces are color coded with their corresponding simulation time steps according to the top color bar. The duration between successive time steps is ~2 s. Also shown in the bottom is the ion energy spectrogram measured by the Galileo PLS during this flyby. The color-coded ion counting rate represents the maximum response at a given E/Q during one spacecraft spin period. The PLS data were obtained from the PPI node of the Planetary Data System. The black dashed line represents the flow energy of heavy ions (with mass/charge = 16) obtained from the simulated flow speed along the Galileo trajectory extracted from a single time step of the simulation when bursty flows are absent near the magnetopause.

nection. More definitive associations will be possible when plasma moments become available.

[22] To illustrate what we propose for interpreting the dynamical changes observed by the Galileo spacecraft near the magnetopause, we show in Figure 5 some representative field lines sampled along the G8 trajectory at one time step in the simulation. As the spacecraft moves in the $+\hat{Y}$ direction, it moves from the region outside of the magnetosphere containing external field lines into the region inside of the magnetosphere, which contains closed field lines. Near the magnetopause where fast flows are seen, the spacecraft encounters reconnected flux tubes ejected from the reconnection sites near the equator, which is below the location of the spacecraft trajectory. The diagram demonstrates that those fast flows identified in the simulation are associated with the reconnection at the magnetopause. That the locations of fast flows being observed vary from one time step to another in our simulation suggests that reconnection in this case is intermittent instead of being steady. For this reason, we attribute the observed boundary oscillations in the G8 flyby data to temporal variations arising from intermittent magnetic reconnection at the magnetopause.

3.2. G28 Flyby

[23] We have discussed the G8 flyby because it is an upstream flyby that passes close to the upstream magnetopause. Galileo made one other upstream pass, the G28 flyby. This flyby was in the southern hemisphere of Ganymede with a lower altitude (~0.34 R_G) at closest approach compared to that of the G8 flyby (~0.61 R_G). Figure 6a shows the 3-D geometry of the flyby trajectory. As for G8, during this pass the spacecraft also moves primarily in the $+\hat{Y}$ direction.

[24] The top four panels in Figure 6b compare the magnetic field measured by the Galileo magnetometer with the simulation results extracted from a single time step. The plots clearly demonstrate that our model does an excellent job of reproducing the observations. The bottom two panels show the counting rates for energetic ions (with energies of 42 ~ 65 keV) and electrons (with energies of 29 ~ 42 keV) observed by the Galileo Energetic Particle Detector (EPD) on the G28 pass. EPD measurements, including the counting rates and pitch angle distributions, have been used to infer magnetic field geometry and to identify different magnetospheric regions by looking for asymmetries associated with loss cones [*Williams et al.*, 1997a, 1997b]. In particular, for

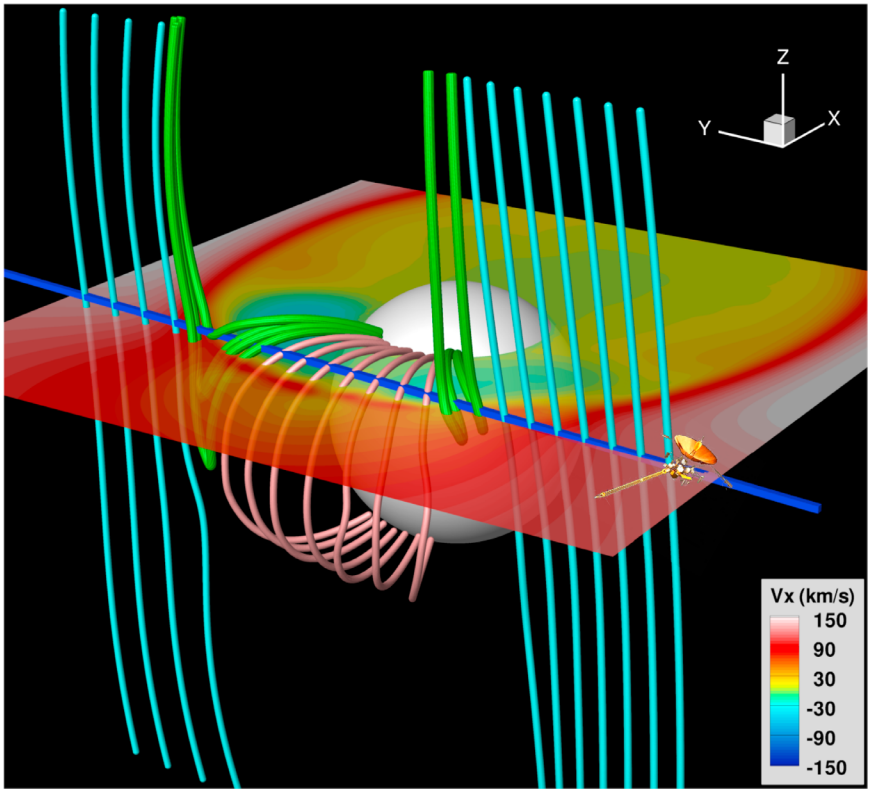

Figure 5. Field lines sampled along the G8 trajectory in the MHD simulation. Color contours of V_x in the XY plane (at Z = 0.7 R_G), which contains the spacecraft trajectory, are also shown to clarify the magnetopause location. Reconnected field lines plotted in green are localized near the magnetopause. The cyan field lines are external field lines and the pink field lines are closed field lines. The Galileo trajectory of the G8 flyby is represented by the blue trace.

the G28 flyby, *Williams* [2001] identified regions of closed field lines inside of Ganymede's magnetosphere where trapped ions and electrons were detected (10:06 ~ 10:13 UT). With results from the global MHD model, we can trace field lines that are encountered along the spacecraft trajectory (shown in Figure 6a) to identify whether they are connected to Ganymede and compare their connectivity with the properties inferred from the EPD measurements. As shown in Figures 6a and 6b, our model results indicate that between 10:06 and 10:13 UT (marked by the green), the spacecraft clearly is on closed field lines, consistent with both the magnetometer observations (strong positive B_z) and the EPD measurements (significant decreases in intensities and trapped-like pitch angle distributions for both energetic ions and electrons). As pointed out by *Williams* [2001], between 10:13 and 10:16 UT (marked with the yellow in Figure 6b), the energetic particle intensities rapidly increase back to ambient Jovian levels, indicating that during this interval the spacecraft probably exits the closed field line region containing trapped particles. The field connectivity cannot be determined from the magnetic field observations alone. However, given the good agreement between the modeled and the observed fields, one can use the simulated global fields to establish the field geometry. As shown in Figure 6a, the field lines extracted from our model suggest that during this interval, Galileo was indeed on open field lines (with one end connected to Ganymede and the other to Jupiter) instead of closed field lines, a result that is consistent with the EPD measurements.

[25] Having validated our model for the G28 pass by comparing simulation results with Galileo observations from multiple instruments, next we focus on dynamical changes of the magnetosphere seen during the G28 flyby as we have shown for the G8 pass in section 3.1. Superposition of the simulated magnetic fields and flow velocities are shown in Figures 7 and 8, respectively. During both the inbound and the outbound magnetopause crossings, the observed magnetic field fluctuates but the amplitudes of the fluctuations are smaller than those observed during the G8 flyby. Our simulated magnetic fields also show variations near the boundary crossings. In particular, for the B_z component during the outbound crossing (10:14 ~ 10:19 UT), the observed field lies well within the range covered by the simulated fields extracted from multiple time steps, suggesting that the observed structure may be caused in part by temporal variations of the magnetopause.

[26] As for the G8 pass, the flows are also variable in the G28 simulation. As shown in Figure 8, fast flows with speed of ~150 km s^{-1} are again present in the vicinity of the magnetopause. In the G28 case, the background magnetic field is tilted by ~45° with respect to the $\hat{Z}$ axis and the shape of the magnetosphere (indicated by the color contours of V_x in the YZ plane in Figure 6a) deviates from symmetry around the $\hat{Z}$ axis. (The magnetosphere is almost symmetric

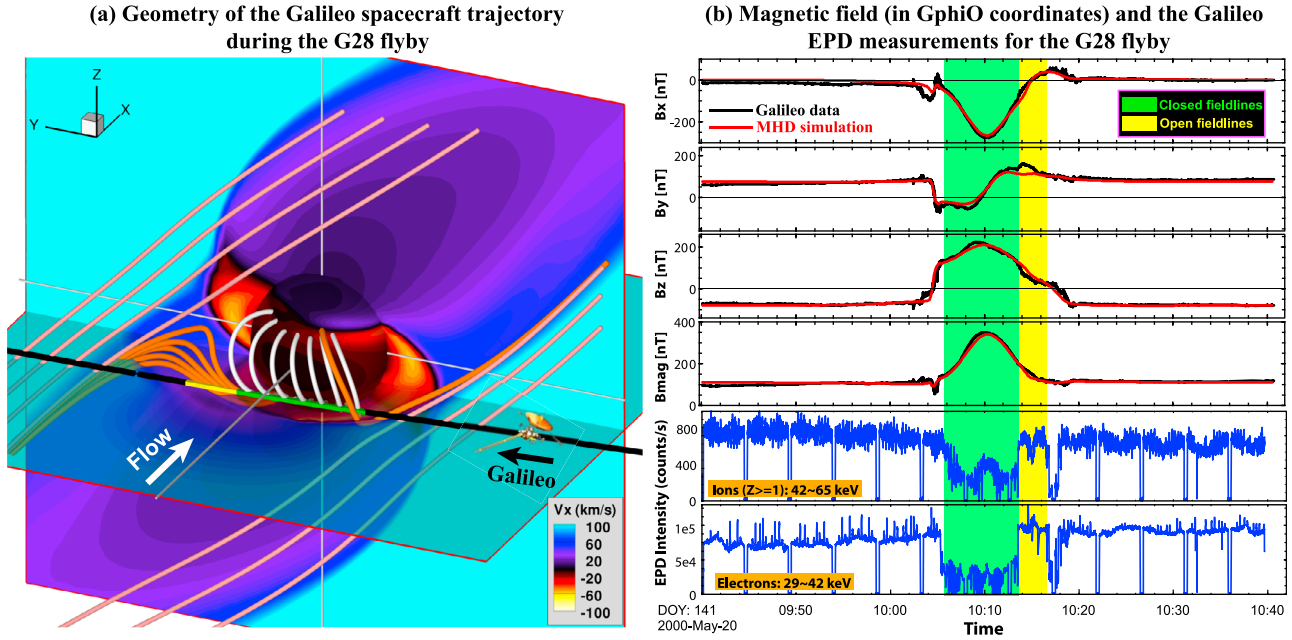

Figure 6. (a) 3-D geometry of the Galileo spacecraft trajectory during the G28 flyby viewed from upstream. Color contours of V_x output from the simulation of the G28 flyby are shown to delineate the magnetopause boundary in both the XY plane (at Z = −0.4R_G) where the spacecraft trajectory approximately lies and the YZ plane (at X = 0). Also plotted are some representative field lines sampled along the trajectory. External field lines are plotted in pink, closed field lines are plotted in white, and open field lines are plotted in orange. The portion of the trajectory where the spacecraft is on closed field lines according to the EPD measurements [*Williams*, 2001] is marked in green, and the portion where the spacecraft exits the closed field line region according to the EPD measurements is marked in yellow. (b) The top four panels show the magnetic field comparisons between the simulation results and the Galileo observations for the G28 flyby. Black solid lines are the spacecraft measurements, and red solid traces are extracted from our MHD simulation. The bottom two panels show the Galileo EPD counting rates for energetic ions (42 ~ 65 keV) and electrons (29 ~ 42 keV), respectively. The EPD data are provided by the PPI node of the Planetary Data System. In Figure 6b, the intervals within the magnetosphere and near the outbound magnetopause crossing are color coded according to the field geometries identified in the simulation: green for closed field lines and yellow for open field lines.

about the $\hat{Z}$ axis for the G8 flyby shown in section 3.1.) As a result, along the spacecraft trajectory, which is approximately parallel to the XY plane, both northward and southward fast flows associated with reconnected flux tubes moving toward high latitudes are encountered (the third panel in Figure 8). In the case of the G8 flyby, which is north of the equator in a magnetosphere not tilted with respect to the $\hat{Z}$ axis, only northward fast flows are seen. Near the magnetopause, the PLS measurements show enhanced ion counting rates at energies well above the ambient flow energy (shown as the black dashed trace), similar to those observed during the G8 flyby. It is plausible to argue that these features are associated with the fast flows caused by bursty reconnection on the magnetopause.

3.3. Bursty Reconnection Under Steady External Conditions

[27] Results presented in sections 3.1 and 3.2 provide information only along the spacecraft trajectory, a one-dimensional line. In order to illustrate the dramatic variations that take place in the vicinity of the magnetopause more completely, we use results from the simulation for the G8 flyby to examine some time sequences of the V_z contours in a two-dimensional plane (XY plane) that contains the spacecraft trajectory (see Figure 9 and Animation S1 of the auxiliary material). In Figure 9, consecutive time frames are separated by 30 s. In the plane of Figure 9, reconnection occurring equatorward will cause fast flows in the northward direction ($+V_z$). Combining all time frames clearly shows that not only the location but also the size and shape of the regions containing fast flows vary from one time to another, indicating that reconnection is not steady but occurs in a bursty manner. If a virtual spacecraft remains at a fixed spatial point located on the upstream magnetopause slightly off the equator, it will observe abrupt changes in plasma conditions, such as enhancement of flow speed and plasma pressure, accompanied by changes in the magnetic field. We find that such changes frequently take place periodically, with periodicities between 20 and 50 s, which is consistent with the periodicities of the observed magnetic fluctuations. Moreover, the dynamic changes in plasma and field conditions, which are manifestations of reconnection, appear in this case to occur almost everywhere on the upstream magnetopause.

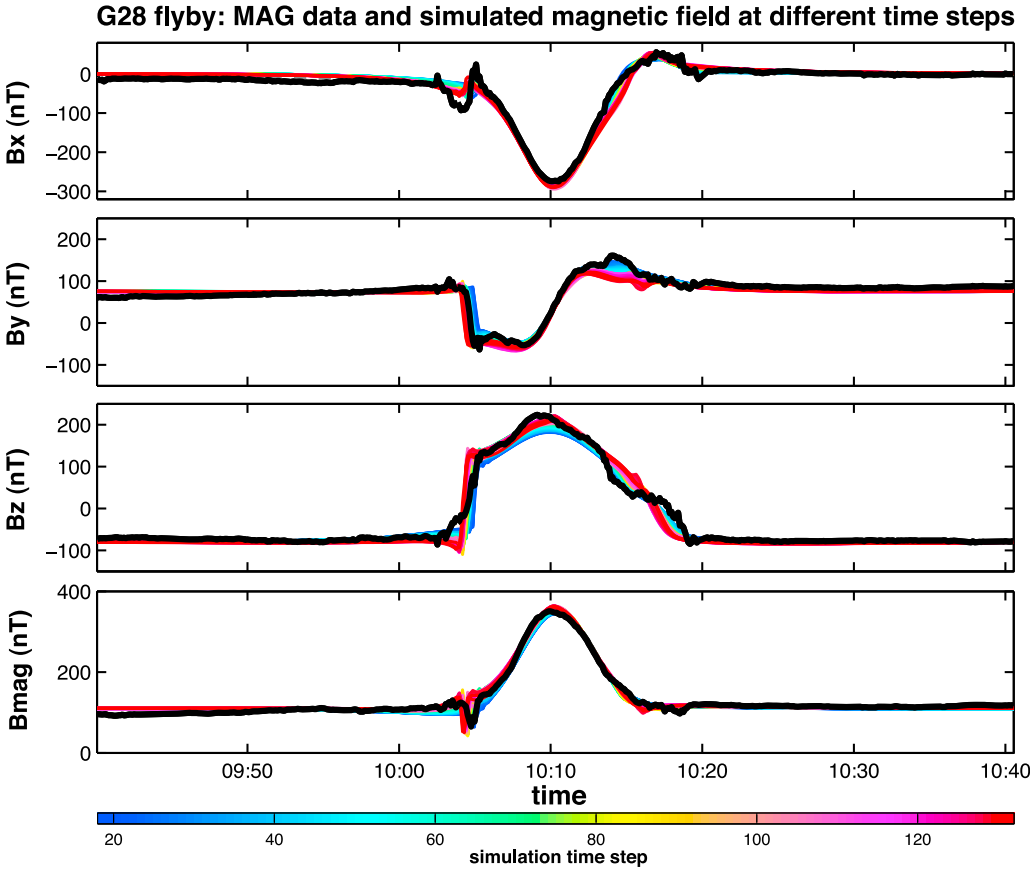

Figure 7. Same as Figure 3 but for the G28 flyby.

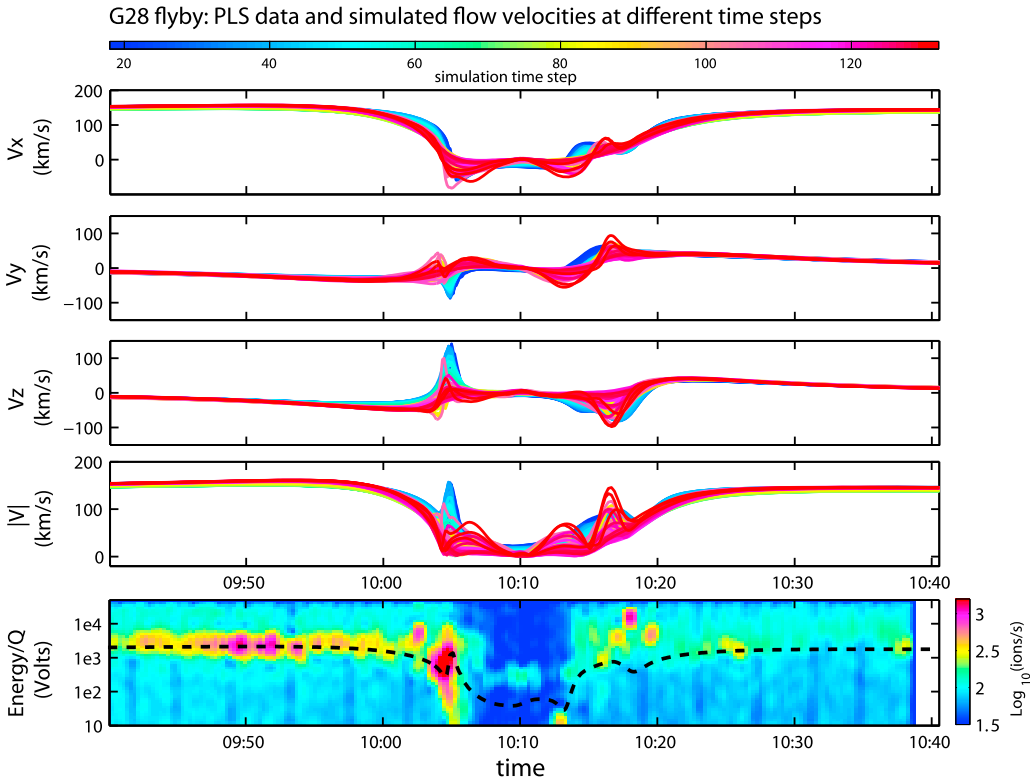

Figure 8. Same as Figure 4 but for the G28 flyby.

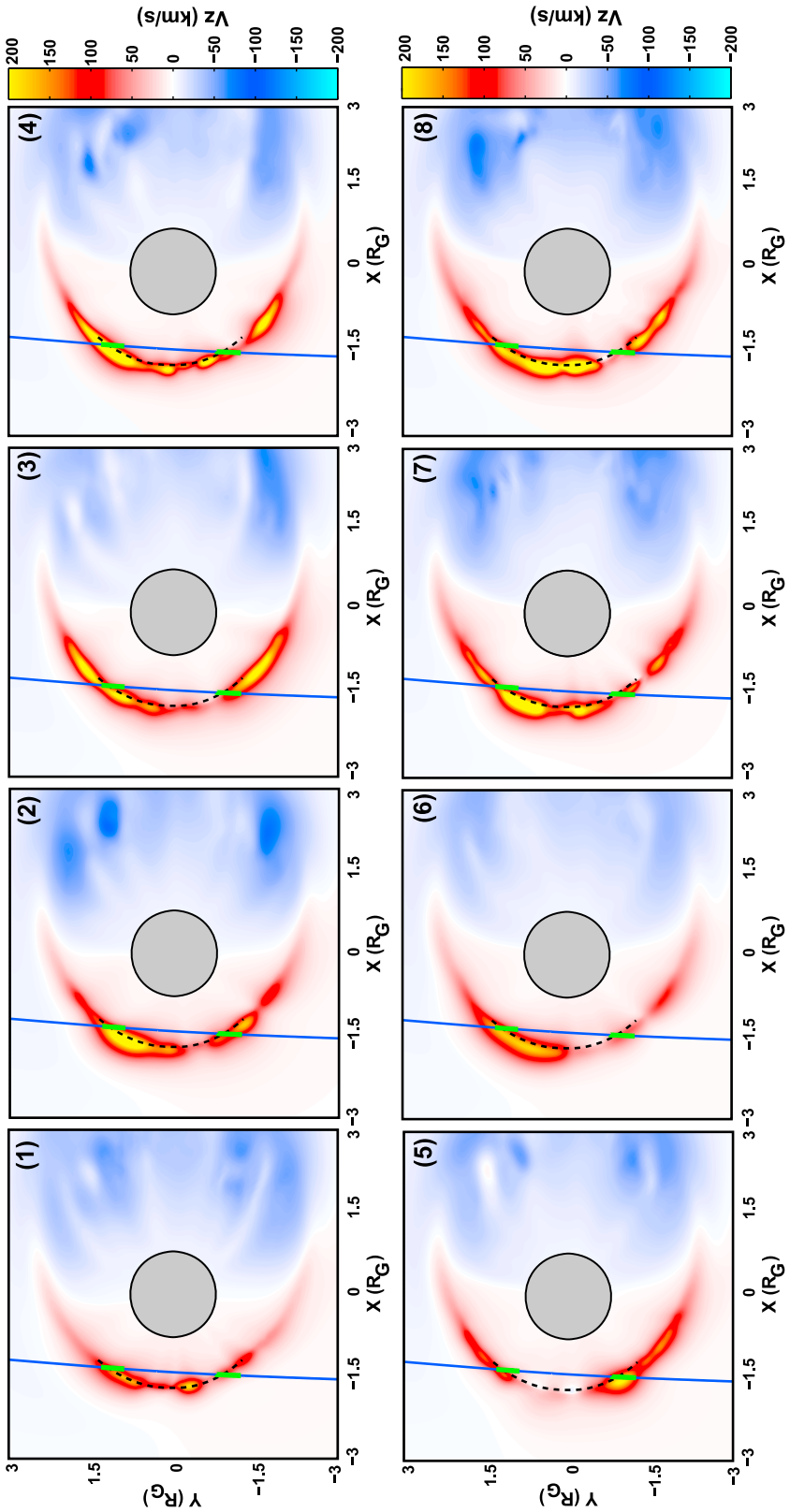

Figure 9. Color contours of V_z in an XY plane (at $Z = 0.7\ R_G$) in which the Galileo spacecraft trajectory (blue trace) lies during the G8 flyby. Results at time steps 1–8 are shown. The time interval between consecutive plots is 30 s. In each plot, two green bars mark the regions along the Galileo trajectory where large magnetic field fluctuations were observed during the inbound and outbound magnetopause crossings.

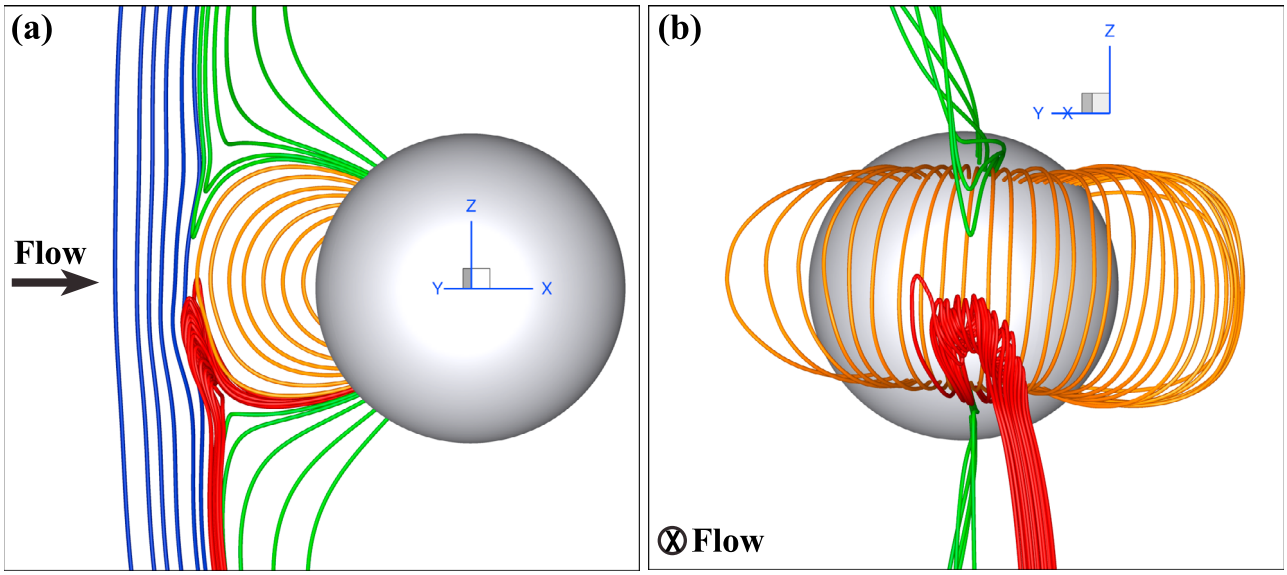

Figure 10. Two perspectives of the 3-D configuration of some representative field lines extracted from one time step of our G8 simulation: (a) an XZ cut in which the incident flow is from left to right; (b) a YZ cut in which the incident flow is flowing into the plane. The connectivity of field lines is color coded as follows. Blue lines are the external Jovian field lines, orange are closed field lines with both ends on Ganymede, and green and red lines are open field lines with only one end on Ganymede.

[28] Similar dynamical changes also are found in the simulations for the conditions of other flybys. In all these simulations, the external plasma and field conditions have been kept fixed in time. Our simulations, therefore, suggest that even under steady external conditions, reconnection is intermittent, a result that is consistent with the presence of fluctuations (previously identified as waves) near the magnetopause encounters as shown in sections 3.1 and 3.2.

4. Comparison of Features of Ganymede's FTEs With Those of Planetary Magnetospheres

[29] In the terrestrial magnetosphere, temporarily and spatially limited reconnection is often observed [*Russell and Elphic*, 1979]. Such localized reconnection events, also called flux transfer events (or "FTEs"), have also been observed in the planetary magnetospheres of Mercury [*Russell and Walker*, 1985; *Slavin et al.*, 2008] and Jupiter [*Walker and Russell*, 1985]. As demonstrated above, bursty reconnection events observed in Ganymede's magnetosphere appear to be impulsive and limited in spatial extent, similar to the features of FTEs found in planetary magnetospheres. Therefore, we also call these localized reconnection events in Ganymede's magnetosphere "FTEs". As an example, we show in Figure 10 the field configuration extracted from one time step of our G8 simulation. Figure 10a provides a snapshot of the general view of the X line geometry on the magnetopause, which separates the external Jovian field lines (in blue) and closed field lines (in orange) with both ends on Ganymede. Reconnected field lines jetting from the reconnection site are depicted by the green and red lines. In particular, the red lines show that some reconnected field lines are in a twisted shape forming flux ropes near the magnetopause. The rope-like geometry of the reconnected field lines, which can be more clearly seen in Figure 10b, appears to have features similar to those inferred for terrestrial FTEs [*Fedder et al.*, 2002; *Raeder*, 2006]. In our global simulations, one can identify the properties of these FTE-like structures, such as their sizes, durations and recurrence rates. It is interesting to compare the features of FTEs seen in Ganymede's magnetosphere with those of planetary magnetospheres. Such a comparative study can extend the parameter regime for the study of reconnection phenomenon. Table 2 lists some general properties of FTEs in four magnetospheres including those of Mercury, Jupiter and Earth. Note that in order to obtain an appropriate comparison between FTE-like features in the Ganymede case and properties of FTEs reported for planetary magnetospheres, which were established based on spacecraft measurements during magnetopause crossings, we measure the properties of Ganymede's FTEs, such as duration and recurrence rate, at a fixed location near the magnetopause in our simulations.

[30] The comparison shows that the absolute size of FTEs varies from one system to another, but the typical sizes of FTEs relative to the body size (R_{body}) are similar (~0.2) for Jupiter, Mercury and Ganymede whereas they are larger at

Table 2. Comparison of FTE-Like Features in a Simulation of Ganymede's Magnetosphere With Properties of FTEs Reported for Planetary Magnetospheres

	Duration	Recurrence Rate	Size (km)	Size[a] (R_{body})	Size[b] (L_{MP})	M_A
Jupiter[c]	<1 min	~4 min	~7000	~0.1	<0.1%	~8
Earth[d]	1 ~ 4 min	~8 min	~6000	~1	5%	~6
Mercury[e]	1 ~ 7 sec	~1 min	240 ~ 1200	0.1 ~ 0.5	10%	~2
Ganymede	5 ~ 10 sec	10 ~ 30 sec	~500	~0.2	5%	~0.7

[a] R_{body} denotes the radius of the body.
[b] L_{MP} denotes the width of the magnetopause.
[c] *Walker and Russell* [1985].
[d] *Rijnbeek et al.* [1984].
[e] *Russell and Walker* [1985] and *Slavin et al.* [2008, 2010].

Earth (~1). When scaled to the width of the magnetopause (L_{MP}), the typical sizes of FTEs are very similar (~5% to 10%) at Earth, Mercury and Ganymede whereas they are much smaller at Jupiter (~0.1%). It also shows that FTEs at Ganymede tend to occur more frequently with much shorter durations than those at Jupiter and Earth. Among the planetary magnetospheres, Mercury's magnetosphere may be the closest analogy to Ganymede's because of their similar spatial sizes and internal field strengths (their internal dipole field strengths differ by roughly a factor of 2). Interestingly, the recurrence rate and duration of FTEs are similar at both Ganymede and Mercury. Since FTEs are localized reconnection events, the properties of FTEs are closely related to reconnection efficiency, which depends on the local plasma and field conditions. There are many factors that can affect reconnection efficiency and hence the properties of FTEs. One controlling factor is thought to be the Alfvén Mach number (M_A) of the incident flow [*Parker*, 1973; *Priest and Forbes*, 2000; *Birn et al.*, 2001]. In general, as M_A becomes larger, reconnection efficiency becomes smaller and the recurrence frequency of FTEs becomes lower. The last column in Table 2 lists the typical M_A values at the objects of interest. It can be seen that the ambient flow at Ganymede typically is sub-Alfvénic and hence has the smallest M_A. This may explain why FTEs occur more frequently at Ganymede than at Mercury and other planets, where the ambient solar wind typically is super-Alfvénic. However, we recognize that more simulations with a wide range of ambient field and plasma parameters are needed in order to clearly identify what controls the reconnection efficiency and the properties of FTEs in a global magnetosphere. Such investigation is beyond the scope of the present paper but will be worth undertaking in the future.

5. Summary and Conclusions

[31] In this paper, we have presented the results from our time-dependent MHD simulations of Ganymede's magnetosphere, with a focus on temporal variations of the magnetosphere on time scales that are comparable to or shorter than the time for the ambient plasma to flow across the magnetosphere. Under constant external conditions, dynamic variations associated with magnetic reconnection on time scales of the order of tens of seconds are found over a large region near the magnetopause in the simulations. In particular, the location of the magnetopause appears to oscillate and bursty flows, along with rapid changes in the field and other plasma properties, are present in the vicinity of the magnetopause. On the two low-latitude passes (G8 and G28) on the upstream side of Ganymede, the Galileo spacecraft detected what appeared to be large-amplitude fluctuations in the magnetic field at the magnetopause crossings. Comparison of the Galileo observations and our global MHD simulations enable us to interpret the observed boundary fluctuations as direct evidence of magnetic reconnection at the magnetopause. The observations and the MHD simulation together suggest that even under steady external conditions, reconnection is predominantly intermittent rather than steady.

[32] The characteristics of bursty reconnection at Ganymede can be compared with properties of FTEs at planetary magnetospheres (Mercury, Earth and Jupiter) to extend the parameter regime available for a study of unsteady reconnection phenomena. Our comparison indicates that the absolute size of FTEs varies from one obstacle to another, the sizes of FTEs relative to the width of the magnetopause are very similar (~5% to 10%) at Mercury, Earth and Ganymede whereas they are much smaller (<0.1%) at Jupiter. FTEs at Ganymede are similar to those at Mercury in terms of the recurrence rate and duration, but tend to occur more frequently with much shorter durations than those at Jupiter and Earth. The low Alfvén Mach number of the ambient flow at Ganymede may explain why FTEs occur more frequently at Ganymede than at Mercury and other planets.

[33] **Acknowledgments.** This research was supported by NASA under grants NNX09AQ54G, NNX08AQ46G, and NNX06AB91G. The authors would like to acknowledge the PDS/PPI for the Galileo PLS and EPD data used in this study. The authors would like to thank the reviewers for their useful comments and suggestions.

[34] Masaki Fujimoto thanks the reviewers for their assistance in evaluating this paper.

References

Anderson, J. D., E. L. Lau, W. L. Sjogren, G. Schubert, and W. B. Moore (1996), Gravitational constraints on the internal structure of Ganymede, *Nature*, *384*, 541–543.

Birn, J., and M. Hesse (2001), Geospace Environment Modeling (GEM) magnetic reconnection challenge: Resistive tearing, anisotropic pressure and hall effects, *J. Geophys. Res.*, *106*, 3737–3750, doi:10.1029/1999JA001001.

Birn, J., et al. (2001), Geospace Environment Modeling (GEM) Magnetic Reconnection Challenge, *J. Geophys. Res.*, *106*, 3715–3719.

Birn, J., et al. (2005), Forced magnetic reconnection, *Geophys. Res. Lett.*, *32*, L06105, doi:10.1029/2004GL022058.

Fedder, J. A., S. P. Slinker, J. G. Lyon, and C. T. Russell (2002), Flux transfer events in global numerical simulations of the magnetosphere, *J. Geophys. Res.*, *107*(A5), 1048, doi:10.1029/2001JA000025.

Frank, L. A., W. R. Paterson, K. L. Ackerson, and S. J. Bolton (1997), Low-energy electrons measurements at Ganymede with the Galileo spacecraft: Probes of the magnetic topology, *Geophys. Res. Lett.*, *24*(17), 2,159–2,162.

Gurnett, D. A., W. S. Kurth, A. Roux, S. J. Bolton, and C. F. Kennel (1996), Evidence for a magnetosphere at Ganymede from plasma-wave observations by the Galileo spacecraft, *Nature*, *384*, 535–537.

Hedstrom, G. W. (1979), Nonreflecting bondary conditions for nonlinear hyperbolic systems, *J. Comp. Phys.*, *30*, 222–237.

Ip, W. H., and A. Kopp (2002), Resistive MHD simulations of Ganymede's magnetosphere: 2. Birkeland currents and particle energetics, *J. Geophys. Res.*, *107*(A12), 1491, doi:10.1029/2001JA005072.

Jia, X. (2009), Ganymede's magnetosphere: Observations and modeling, Ph.D. thesis, Univ. of Calif., Los Angeles.

Jia, X., R. J. Walker, M. G. Kivelson, K. K. Khurana, and J. A. Linker (2008), Three-dimensional MHD simulations of Ganymede's magnetosphere, *J. Geophys. Res.*, *113*, A06212, doi:10.1029/2007JA012748.

Jia, X., R. J. Walker, M. G. Kivelson, K. K. Khurana, and J. A. Linker (2009), Properties of Ganymede's magnetosphere inferred from improved three-dimensional MHD simulations, *J. Geophys. Res.*, *114*, A09209, doi:10.1029/2009JA014375.

Kivelson, M. G., K. K. Khurana, C. T. Russell, R. J. Walker, J. Warnecke, F. V. Coroniti, C. Polanskey, D. J. Southwood, and G. Schubert (1996), Discovery of Ganymede's magnetic field by the Galileo spacecraft, *Nature*, *384*, 537–541.

Kivelson, M. G., J. Warnecke, L. Bennett, S. Joy, K. K. Khurana, J. A. Linker, C. T. Russell, R. J. Walker, and C. Polanskey (1998), Ganymede's magnetosphere: Magnetometer overview, *J. Geophys. Res.*, *103*, 19,963–19,972.

Kivelson, M. G., K. K. Khurana, and M. Volwerk (2002), The permanent and inductive magnetic moments of Ganymede, *Icarus*, *157*, 507–522.

Kivelson, M. G., F. Bagenal, W. S. Kurth, F. M. Neubauger, C. Paranicas, and J. Saur (2004), Magnetospheric interactions with satellites, in *Jupiter: The Planet, Satellites and Magnetosphere*, edited by F. Bagenal et al., pp. 513–536, Cambridge Univ. Press, Cambridge, U. K.

Kopp, A., and W. H. Ip (2002), Resistive MHD simulations of Ganymede's magnetosphere: 1. Time variabilities of the magnetic field topology, *J. Geophys. Res.*, *107*(A12), 1490, doi:10.1029/2001JA005071.

Linker, J. A., M. G. Kivelson, and R. J. Walker (1991), A three-dimensional MHD simulation of plasma flow past Io, *J. Geophys. Res.*, *96*, 21,037–21,053, doi:10.1029/91JA02132.

Linker, J. A., Z. Mikić, D. A. Biesecker, R. J. Forsyth, S. E. Gibson, A. J. Lazarus, A. Lecinski, P. Riley, A. Szabo, and B. J. Thompson (1999), Magnetohydrodynamic modeling of the solar corona during whole sun month, *J. Geophys. Res.*, *104*, 9809–9830.

Mikić, Z., and J. A. Linker (1994), Disruption of coronal magnetic field arcades, *Astrophys. J.*, *430*, 898–912.

Otto, A. (2001), Geospace Environment Modeling (GEM) magnetic reconnection challenge: MHD and Hall MHD-constant and current dependent resistivity models, *J. Geophys. Res.*, *106*, 3751–3758, doi:10.1029/1999JA001005.

Parker, E. N. (1973), The reconnection rate of magnetic fields, *Astrophys. J.*, *180*, 247–252, doi:10.1086/151959.

Paty, C., and R. Winglee (2006), The role of ion cyclotron motion at Ganymede: Magnetic morphology and magnetospheric dynamics, *Geophys. Res. Lett.*, *33*, L10106, doi:10.1029/2005GL025273.

Priest, E., and T. Forbes (Eds.) (2000), *Magnetic Reconnection: MHD Theory and Applications*, Cambridge Univ. Press, New York.

Raeder, J. (2006), Flux transfer events: 1. Generation mechanism for strong southward IMF, *Ann. Geophys.*, *24*, 381–392.

Rijnbeek, R. P., S. W. H. Cowley, D. J. Southwood, and C. T. Russell (1984), A survey of dayside flux transfer events observed by ISEE 1 and 2 magnetometers, *J. Geophys. Res.*, *89*, 786–800, doi:10.1029/JA089iA02p00786.

Russell, C. T., and R. C. Elphic (1979), ISEE observations of flux transfer events at the dayside magnetopause, *Geophys. Res. Lett.*, *6*, 33–36, doi:10.1029/GL006i001p00033.

Russell, C. T., and R. J. Walker (1985), Flux transfer events at Mercury, *J. Geophys. Res.*, *90*, 11,067–11,074, doi:10.1029/JA090iA11p11067.

Schnack, D. D., D. C. Barnes, Z. Mikić, D. S. Harned, and E. J. Caramana (1987), Semi-implicit magnetohydrodynamic calculations, *J. Comp. Phys.*, *70*, 330–354.

Schubert, G., K. Zhang, M. G. Kivelson, and J. D. Anderson (1996), The magnetic field and internal structure of Ganymede, *Nature*, *384*, 544–545.

Slavin, J. A., et al. (2008), Mercury's magnetosphere after MESSENGER's first flyby, *Science*, *321*, 85–89, doi:10.1126/science.1159040.

Slavin, J. A., et al. (2010), MESSENGER observations of large flux transfer events at Mercury, *Geophys. Res. Lett.*, *37*, L02105, doi:10.1029/2009GL041485.

Walker, R. J., and C. T. Russell (1985), Flux transfer events at the Jovian magnetopause, *J. Geophys. Res.*, *90*, 7397–7404, doi:10.1029/JA090iA08p07397.

Williams, D. J. (2001), Ganymede's ionic radiation belts, *Geophys. Res. Lett.*, *28*(19), 3,793–3,796.

Williams, D. J., et al. (1997a), Energetic particle signatures at Ganymede: Implications for Ganymede's magnetic field, *Geophys. Res. Lett.*, *24*(17), 2,163–2,166.

Williams, D. J., B. Mauk, and R. W. McEntire (1997b), Trapped electrons in Ganymede's magnetic field, *Geophys. Res. Lett.*, *24*(23), 2,953–2,956.

X. Jia and M. G. Kivelson, Department of Atmospheric, Oceanic and Space Sciences, University of Michigan, Ann Arbor, MI 48109-2143, USA. (xzjia@umich.edu)

K. K. Khurana and R. J. Walker, Institute of Geophysics and Planetary Physics, University of California, Los Angeles, CA 90095, USA.

J. A. Linker, Predictive Science, Inc., 9990 Mesa Rim Rd., Ste. 170, San Diego, CA 92121, USA.